American Journal of Botany 92(2): 252–261. 2005.

GENE FLOW AND FINE-SCALE GENETIC STRUCTURE IN A WIND-POLLINATED TREE SPECIES, *QUERCUS LOBATA* (FAGACEAEE)[1]

CYRIL DUTECH,[2,5] VICTORIA L. SORK,[2] ANDREW J. IRWIN,[3,6]
PETER E. SMOUSE,[3] AND FRANK W. DAVIS[4]

[2]Department of Ecology and Evolutionary biology, University of California Los Angeles, P.O. Box 951605, Los Angeles, California 90095-1605 USA; [3]Department of Ecology, Evolution and Natural Resources, Cook College, Rutgers University, New Brunswick, New Jersey 08901-8551 USA; and [4]Donald Bren School of Environmental Science and Management, University of California Santa Barbara, California 93106 USA

California Valley oak (*Quercus lobata*), one of the state's most distinctive oak species, has experienced serious demographic attrition since the 19th century, due to human activities. Recent estimates of pollen dispersal suggest a small reproductive neighborhood. Whether small neighborhood size is a recent phenomenon, a consequence of reduced gene flow caused by demographic changes, or whether it has been historically restricted, remains unclear. To examine this question, we have characterized the spatial genetic structure of $N = 191$ *Q. lobata* individuals, spread over an area of 230 ha, using eight microsatellite loci. The observed autocorrelogram suggests an historical standard deviation of gene flow distance of about 350 m per generation, higher than contemporary pollen dispersal estimates. To determine whether our estimates were affected by strong prevailing winds from the west–northwest, we developed and utilized a novel anisotropic autocorrelation analysis. We detected no more than a hint of anisotropy, and we concluded that adult spatial structure is indicative of strong historical signature of ''isolation by distance.'' This historical estimate provides a useful reference value against which to gauge the future gene flow consequences of ongoing anthropogenic disturbance.

Key words: bearing correlogram; California oak; genetic autocorrelation analysis; microsatellite; pollen and seed dispersal; tree species; wind direction.

Gene flow is a major evolutionary force, homogenizing genetic variation across populations by moving alleles from one population to another (Wright, 1951; Slatkin, 1987) and governing the effective size of the local neighborhood (sensu Wright, 1943). Recently, conservation biologists have become concerned about the impact of human disturbance on gene flow because processes such as fragmentation and demographic attrition can increase genetic isolation and decrease local population size in a manner that could jeopardize the viability of the remaining populations (Ledig, 1988, 1992; Ellstrand and Elam, 1993). Many studies of plant species have focused on contemporary pollen movement because pollen dispersal is often considered to have greater spatial scale than seed dispersal (Ennos, 1994) and because it is easier to study (Sork et al., 1999; Smouse and Sork, 2004). Some studies have shown that pollen-mediated gene flow increases across fragmented landscapes, as for tropical *Ficus* species with specialized pollinator systems (Nason and Hamrick, 1997) and for Brazilian *Dinizia excelsa*, where fragmentation has led to a shift in pollinators from specialist native forest bees, flying relatively short distances, to nonnative generalist Africanized honey bees, which fly great distances (Dick et al., 2003). Other studies have observed that fragmentation can lead to an increase in inbreeding and a reduction in gene flow for the relict individuals in forest fragments, as for the tropical dry forest dominant, *Enterolobium cyclocarpum* (Rocha and Aguilar, 2001). In all of these cases, anthropogenic disturbance has caused changes in the patterns of contemporary gene flow that will influence the future genetic structure of these populations.

Here, we are concerned with *Quercus lobata* Neé (henceforth Valley oak), one of California's signature species. Valley oak is a canopy tree species, generally found on deep loamy soils, below 600 m of elevation (Pavlik et al., 1991). Along with *Q. agrifolia* and *Q. douglasii*, it is one of the more common tree species of the savanna oak community from the noncoastal lowlands, between Shasta Lake and the Santa Monica Mountains. It is also the most threatened of California's oak species, with a distribution that has been impacted seriously by continuing agricultural development, and with local populations becoming progressively sparser, due to ongoing demographic attrition (Griffin, 1971; Brown and Davis, 1991). This savanna oak occurs naturally in low densities (2–10 trees/ha), but a further consequence of progressive demographic thinning is that individuals may become reproductively isolated into small, sparse populations, among which pollen movement may become limited. From two seasons of study, using the TWOGENER pollen pool structure analysis of Smouse et al. (2001), we estimate that the standard deviation of pollination distance can vary from 50 to 88 m, the average distance can vary between 64 and 110 m, and the effective number of pollen donors per maternal adult ranges from 4 to 18 individuals (Sork et al., 2002a; Austerlitz et al., 2004). The emerging story

[1] Manuscript received 27 February 2004; revision accepted 12 October 2004.

The authors thank F. Austerlitz, J. F. Fernandez, O. Hardy, and R. Westfall for helpful comments on the manuscript. We also wish to thank D. Grivet, B. Kuhn, D. Tomerlin, and M. Williams for help with the field collections, and D. Grivet, C. Prenger, and D. Tomerlin for help with the lab work. C. D. and V. L. S. were supported by NSF-DEB-0089445, NSF-DEB-0242422, and UCLA, A. J. I. by the Natural Sciences & Engineering Research Council of Canada, P. E. S. by NSF-BSR-0089238 and NJAES/USDA-17111, and F. D. by NSF-DEB-0089495.

[5] Present address: Institut National de la Recherche Agronomique—Bodeaux,Unité Mixte de Recherche BIOGECO, Laboratoire de Pathologie Forestière Domaine de la Grande Ferrade-BP81 33883 Villenave d'Ornon, France (e-mail address: cdutech@bordeaux.inra.fr).

[6] Present address: Department of Biology, College of Staten Island–CUNY, Staten Island, New York 10314 USA.

for Valley oak is that the contemporary pollination neighborhood ranges in size from 3 to 10 ha.

An understanding of contemporary pollen movement would be enhanced by comparison with a historically relevant reference value, which latter should be reflected in the genetic structure of the extant adults themselves. If Valley oak has historically exhibited restricted pollen movement, and if a larger proportion of seeds are dispersed by rodents with restricted seed dispersal, as presumed for other oak species (Ducousso et al., 1993), we might anticipate that Valley oak should exhibit a strong and significant spatial genetic structure. Neighboring individuals would be more likely than distant individuals to share alleles (i.e., ''isolation by distance'' pattern (IBD); Wright, 1943; Malécot, 1950; Rousset, 2000). Such a pattern can be detected in plant populations by genetic autocorrelation analysis, describing the relationship between pairwise genetic affinity of individuals and pairwise interindividual distance (Heywood, 1991; Hardy and Vekemans, 1999). This method can be used to estimate the scale of gene movement (Hardy and Vekemans, 1999; Rousset, 2000). Assuming that genetic markers used in the analysis are not affected by natural selection, regression analysis yields an estimate of effective population size, $N_e = 4\pi D_e\sigma^2$, where D_e is the effective reproductive population density and σ^2 is the second moment of the dispersal distance, measured from parent to offspring, because spatial genetic structure is assumed to reflect the net balance between gene flow and genetic drift. Given an extraneous estimate of D_e, we can extract an estimate of σ, the standard deviation of successful propagule dispersal (with seed and pollen flow combined). An analysis of fine-scale genetic structure should reflect the cumulative historical scale of propagule flow, which can be compared with our independently acquired estimate of contemporary pollen movement, to determine whether contemporary and historical processes have been operating on similar scales.

Because Valley oak is wind-pollinated, we might expect wind patterns that have been consistent over many generations could have shaped spatial genetic structure among surviving adults. Our particular study population, on the Sedgwick Reserve in Santa Barbara County, is located in a region that exhibits a predominant west–northwest wind direction (Dorman and Winant, 2000). Preferential pollen movement along the major wind axis could create differing degrees of relationship between pairs of individuals, depending on whether they are separated along the major axis of pollen flow or across it. Such directional asymmetry in genetic affinity (usually called ''anisotropy'') could affect the analysis of spatial genetic structure, because most autocorrelation analyses of propagule flow have assumed ''isotropy'' or radial symmetry (Tufto et al., 1997). At Sedgwick Reserve, the prevailing winds are strong enough that we might expect them to have favored genetic relatedness among individuals along the predominant wind axis, which should produce a slow (but steady) decline of relatedness with distance. Perpendicular to the wind axis, genetic autocorrelation might be significant among close neighbors, as a consequence of localized seed movement, but genetic relatedness should decrease strongly beyond a relatively short distance, because of a low pollen flow in that direction. We can therefore expect that the slope of the genetic correlogram should be steeper across (perpendicular to) the wind axis than along it. The question is whether wind-induced anisotropy of pollen flow has imposed a lasting signature of directional asymmetry on the adult structure in our population.

Here, we will assess whether the genetic signature of the adult population reveals a historical scale of gene movement that is comparable with contemporary pollen movement, assuming that seed dispersal is much more restricted than pollen dispersal (as is common in many tree species; Ennos, 1994). Our objective is to examine the pattern of genetic affinities among $N = 191$ adults at Sedgwick Reserve, using a collection of eight microsatellite loci. This analysis allows us to address three specific questions: (1) Is there significant autocorrelation in the Valley oak population at Sedgwick Reserve? (2) What is the scale of gene flow inferred by Rousset's method (2000)? (3) Does our population exhibit anisotropic autocorrelation in a manner consistent with predictions based on the predominant wind direction at the study site?

MATERIALS AND METHODS

Study site and sampling regime—The study site is located at the Sedgwick Reserve, along Figueroa Creek (34°42′ N, 120°02′ W), 10 km northeast of Santa Ynez (Santa Barbara County, California, USA). Sedgwick Reserve (2380 ha) is part of the University of California Natural Reserve System, administered by the University of California at Santa Barbara. Valley oaks at our study site occupy deep alluvial soils on the valley floor and adjacent hill slopes, at elevations ranging from 300 to 400 m above sea level (Fig. 1). The valley is oriented roughly north-south and is bounded by ridges ranging in elevation from 440 to 475 m above sea level.

The current stem density of Valley oak averages about 1.19 adult trees/ha at Figueroa Creek and all individuals are greater than 40 cm diameter at breast height (dbh), except for a single 2 cm dbh sapling. This relict population has experienced steady demographic attrition throughout the 19th and 20th centuries, due to human activities (Pavlik et al., 1991). At Figueroa Creek, we estimate a 20% loss of trees between 1944 and the present, based on analysis of archival air photos (Sork et al., 2002a). It is not possible to reconstruct the adult densities, prior to occupation of the area by Mexican ranchers in the mid-19th century, but based on current maximum densities on comparable soils in the region, it is conceivable that adult densities were 1.5–2.5 times higher in the mid-19th century than they are today.

In the spring and summer of 2002, we sampled leaves from the majority of adult individuals ($N = 191$) along Figueroa Creek, including the slopes on both sides of the canyon (Fig. 1). A spatial buffer of 200 m around all sampled trees encompasses a 230-ha region that includes an additional (but ungenotyped) 123 adults. Assuming low gene flow in *Q. lobata* (see INTRODUCTION), genetic clustering (spatial genetic structure) was expected among neighboring individuals. Our sampling goal was to include individuals separated by small, intermediate and longer distances, rather than to exhaustively sample all individuals within the study area. Tree density in the buffered area is 1.36 trees/ha. After collection, leaves were stored at −80°C in the laboratory, pending genetic analysis.

DNA analysis—We extracted total DNA from 30–40 mg of frozen leaves from each individual, using a cetyltrimethylammonium bromide (CTAB) buffer and liquid nitrogen, following the method described in Sork et al. (2002a). We utilized a battery of eight unlinked microsatellite loci, QrZAG11, QrZAG20, QpZAG1/5, QpZAG9, QpZAG36, and QpZAG110, developed by Steinkellner et al. (1997) for *Q. robur* and *Q. petreae*, MSQ4, developed by Dow et al. (1995) for *Q. macrocarpa*, and Qm50, developed by Isagi and Suhandono (1997) for *Q. myrsinifolia*. We used polymerase chain reaction (PCR) and visualization methods described by Sork et al. (2002a).

Wind regime—Due to latitude, regional topography and coastal location, prevailing winds in the Santa Ynez Valley are from the west–northwest (Dorman and Winant, 2000). The Sedgwick Reserve has maintained a weather station 900 m from the center of our study population since 1997. We analyzed hourly average wind speed and direction for the main flowering period of 1 March to 30 April (Fairley and Batchelder, 1986) for the years 1997–2003. Conditions for pollen dispersal are best during the late morning through

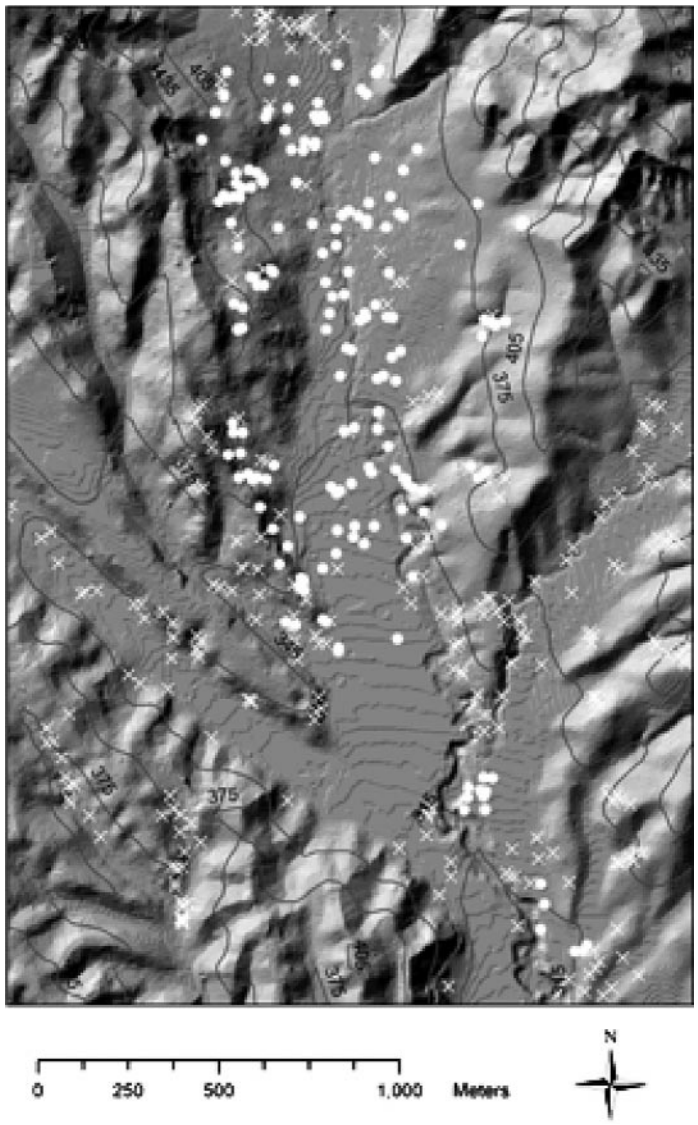

Fig. 1. Contour map of Valley oak study region at Sedgewick Reserve, Santa Barbara County, California, USA. Sampled Valley oak (*Quercus lobata*) trees are indicated with circles, unsampled adults are indicated with ×.

early evening hours (1100–1900 hours), when air temperature increases, relatively humidity decreases, and wind velocity increases 2–4 fold at the study site (F. W. Davis, unpublished data). Because these conditions certainly favor pollination and should have the strongest impact on pollen dispersal, estimates of average wind speed and the distribution of hourly average wind directions (the wind rose) were estimated for the period between 1100 and 1900 hours.

Genetic data analysis*—Hardy-Weinberg*—As background for our results, we estimated observed (H_o) and expected heterozygosity (H_e, following Nei, 1987), number of alleles (N_{all}), and inbreeding coefficient (F_{IS}, following Weir and Cockerham, 1984) for each of the eight microsatellite loci. We performed exact tests for Hardy-Weinberg proportions for the complete battery of eight loci and for each of the eight microsatellite loci, separately. Similarly, we performed exact tests for gametic disequilibrium between each pair of loci. We used Genepop version 3.1d (Raymond and Rousset, 1995) for all of these tests.

Kinship—We estimated the relatedness between pairs of individuals, based on Nason's kinship coefficient (*r*), as described in Loiselle et al. (1995), and defined as a ratio of probabilities of identity by descent (for details see Hardy, 2003). Assuming migration-drift equilibrium, the impact of mutation at small spatial scales is negligible, relative to that of gene flow, and the ratio of probabilities of identity in state is similar to that of probabilities of identity by descent (Rousset, 1996). Using the formula from the SPAGeDi software (Hardy and Vekemans, 2002), we estimated the kinship coefficient for the *i*th and *j*th individuals, formally defined over all alleles and loci, as

$$r_{ij} = \frac{\sum_{k=1}^{K} (p_{ik} - \bar{p}_{\cdot k})(p_{jk} - \bar{p}_{\cdot k})}{\sum_{k=1}^{K} \bar{p}_{\cdot k}(1 - \bar{p}_{\cdot k})} + \frac{1}{(2n - 1)}, \quad (1)$$

where $\bar{p}_{\cdot k}$ the mean frequency of the *k*th allele in the sampled population, and p_{ik} and p_{jk} are the frequencies of the *k*th allele in the *i*th and *j*th individuals (taking the values 0, 0.5 and 1, respectively, for homozygotes lacking the *k*th allele, heterozygotes having one copy of the *k*th allele, and homozygotes for the *k*th allele), and where *n* is the sample size. The second term of the equation corrects for finite sampling. Average kinship coefficients were estimated for each distance interval, considering all pairs of individuals separated by a spatial distance included in that interval. For the *h*th distance interval, this is formally accomplished by computing

$$r^{[h]} = \frac{\sum_{i \neq j}^{N} w_{ij}^{[h]} r_{ij}}{\sum_{i \neq j}^{N} w_{ij}^{[h]}}, \quad (2)$$

where $w^{[h]}_{ij}$ takes the value 1 if the distance between the *i*th and *j*th individuals falls within the [*h*]th distance interval, and takes the value 0 otherwise.

Isotropic autocorrelation—A linear decrease of kinship coefficient with the logarithm of spatial distance is expected if gene flow follows a process of isolation by distance in two dimensions (Rousset, 1997, 2000). We thus computed average kinship coefficients for individuals separated by various degrees of spatial isolation. The natural logarithm of the maximum distance of the first distance class is 3.5 (i.e., all individuals are separated by from 0 to 33 m), and the logarithmic increment between successive classes is 0.50. Each estimate of $r^{[h]}$ was plotted against its intertree distance interval to produce a correlogram, from which we can visualize the decay of kinship with distance. We estimated the probability that the average kinship coefficient of a particular distance class was significantly different from that obtained from a genetically randomized population (no spatial structure) with 1000 permutational shuffles of the spatial coordinates of the individuals themselves. The difference over all the distance classes between the spatial genetic structure of Valley oak at Sedgwick Reserve and a genetically randomized population was also tested by a *t* test, defined as:

$$T = \sqrt{\sum_{h=1}^{H} \frac{(r^{[h]} - 0)^2}{\tilde{\sigma}^2_{[h]}}}, \quad (3)$$

where $\tilde{\sigma}^2_{[h]}$ is the estimated variance of the estimated correlation, $r^{[h]}$, determined by permuting the sampled individuals (1000 permutations) among locations. The observed *t* value is compared with an empirically generated null distribution, obtained by permuting the spatial coordinates of the *N* individuals, and the ''tail probability'' is assessed as the number of random trial values of *T* that equal or exceed that observed value.

Regression analysis—Rousset (2000) introduced an approach that allows extraction of information on the scale of gene movement that creates fine spatial genetic signature, by extending his model of genetic relationships among populations (Rousset, 1997) to the relatedness between individuals within single populations. Within populations, Rousset (2000) showed that, for an isolation-by-distance model in two-dimensional habitat with neutral loci, we should expect a linear regression of the relatedness coefficient between a pair of individuals, on the natural logarithm of geographic distance. The slope of the regression provides an estimate of $1/4\pi D_e\sigma^2$, where D_e is the effective reproductive population density and σ^2 is the second moment of the dispersal distance, measured from parent to offspring. Thus, $4\pi D_e\sigma^2$ can be related to neighborhood size (N_e), as defined by Wright (1951), but in Rousset's method, this product is essentially independent of the dispersal function and only estimates the spatial scale of gene flow. Vekemans and Hardy (2004) have extended this approach and proposed a slightly different way of estimating dispersal parameters for spatial genetic structure. Under certain conditions, their ''S_p'' statistic can be used to estimate $1/4\pi D_e\sigma^2$. This statistic provides a means of comparing estimates of dispersal parameters from fine-scale genetic structure with those derived from direct measures. Furthermore, S_p has proven to be a convenient parameter for assessing the degree of spatial genetic structure and for comparing such structure across species, independent of the sampling scheme (see Vekemans and Hardy, 2004).

We estimated the S_p statistic as $b_k/(r^{[1]} - 1)$, where b_k is defined as the estimated regression slope of the Loiselle et al. (1995) kinship coefficient on the logarithm of spatial distance and $r^{[1]}$ is the average kinship coefficient between pairs of individuals within the first distance class, respectively (Hardy and Vekemans, 1999; Vekemans and Hardy, 2004). The significance of the kinship regression on the natural logarithm of spatial distance (i.e., the test for isolation by distance) was obtained by permuting individual locations and comparing the observed b_k value with the frequency distributions obtained by permutation (Rousset, 1997; Hardy and Vekemans, 2002) for each locus and for the multilocus estimate. The standard error of b_k was obtained by jackknifing genetic loci (Hardy and Vekemans, 2002). Thus, the extent of gene flow (as measured by the σ parameter) can be estimated under the assumption of an effective population density D_e.

Inclusion of both the very proximal and very distal pairs can bias the σ estimate (Rousset, 1997, 2000). In order to remove the possible effect of these pairs on the σ estimate, we used an iterative method developed by Fenster et al. (2003). A first σ estimate ($\hat{\sigma}$) is obtained by including all pairs of individuals. Based on this first estimate, all pairs outside the interval ($\hat{\sigma} < d_{ij} < 20\ \hat{\sigma}$) are discarded from the new regression, yielding a revised estimate, $\hat{\sigma}$. This procedure is repeated until $\hat{\sigma}$ converges, along with the range of distances between pairs of individuals used for the regression (i.e., $\hat{\sigma}$ to $20\ \hat{\sigma}$). Using the standard error of b_k (SE_b), obtained by jackknifing among loci (Hardy and Vekemans, 2002), we constructed a 95% confidence interval (CI) of N_e as $(r^{[1]} - 1)/(b_k \pm 2\ SE_b)$. Because $\hat{\sigma} = \sqrt{N_e/(4\pi D_e)}$, the 95% CI of $\hat{\sigma}$ was estimated from the upper and lower limits of the 95% CI of N_e. We extracted all of the estimates and conducted all of the isotropic hypothesis tests with the autocorrelation program SPAGeDi, Version 1.1 (Hardy and Vekemans, 2002; http://www.ulb.ac.be/sciences/lagev).

Anisotropic autocorrelation—If wind direction has an important effect on pollination and on spatial genetic structure, we would predict that the correlogram should decrease more slowly with distance along the main wind azimuth, and the correlogram with the sharpest slope for the shorter distance classes should be at right angles to that first axis (across the prevailing wind vector). To assess the effect of wind on spatial structure, we conducted a directional autocorrelation analysis, for which we used minor modifications of a technique developed by Rosenberg (2000). Building on earlier work by Oden and Sokal (1986), Rosenberg (2000) introduced a novel directional autocorrelation analysis for univariate data. Smouse and Peakall (1999) have pointed out that single-allele (univariate) autocorrelation results have large statistical variance, but that analogous multi-allele/multilocus (multivariate) analysis reduces stochastic noise, so we have developed such an approach here.

Rosenberg's (2000) method provides an analysis for any direction, adjusting the weights for the difference between the directional angle between two individuals, denoted α_{ij}, and the azimuth along which we assess spatial pattern, denoted θ. Specifically, we define

$$w^{[h]}_{ij}(\theta) = w^{[h]}_{ij} \cdot \cos^2(\theta - \alpha_{ij}), \quad (4)$$

where $w^{[h]}_{ij}(\theta)$ remains 0 if the *ij* pair does not fall within the *h*th distance interval, but $w^{[h]}_{ij}(\theta)$ varies continuously between 0 and 1 if the *ij* pair falls within the *h*th distance interval, the exact value depending on the angular displacement (α_{ij}) between the two individuals, as well as the azimuth (θ) being considered. If $\theta = \alpha_{ij}$ (the angular displacement of the two individuals is the same as the azimuth being considered), $w^{[h]}_{ij}(\theta) = 1$, but if $\theta = \alpha_{ij} \pm 90°$ (the two individuals have an angular displacement that is perpendicular to the azimuth being considered), $w^{[h]}_{ij}(\theta) = 0$. The method ''weights'' the distance between the two individuals by the difference between their angular displacement and the azimuth being considered.

For any given distance class, we can describe the changing pattern of $r^{[h]}(\theta)$ as we navigate around the circle, with θ measured as the clockwise angular displacement from 0° (true North). We computed a correlogram for each of 180 trial azimuths (every 1°), portraying the relationships for successive distance classes. We should expect the autocorrelation coefficients to decrease most rapidly with increasing distance class along the angle of greatest pattern (θ_{max}) and to decrease more slowly with increasing distance class across the angle of greatest pattern ($\theta_{min} = \theta_{max} \pm \frac{1}{2}\pi$), by virtue of the geometric construction of the angular weights. Evaluation of the difference in the correlograms along (and across) the primary wind direction should also tell us how well (or poorly) the direction of the wind accounts for the pattern of any anisotropy we encounter.

In addition to the usual test of the hypothesis that the isotropic correlogram represents a significant departure from the null hypothesis of no autocorrelation ($r^{[h]} = 0$ for all distance intervals, [*h*]; see Smouse and Peakall, 1999), we have added a statistically independent test of the difference between the correlogram along any particular azimuth (θ) and that at right angles ($\theta \pm$

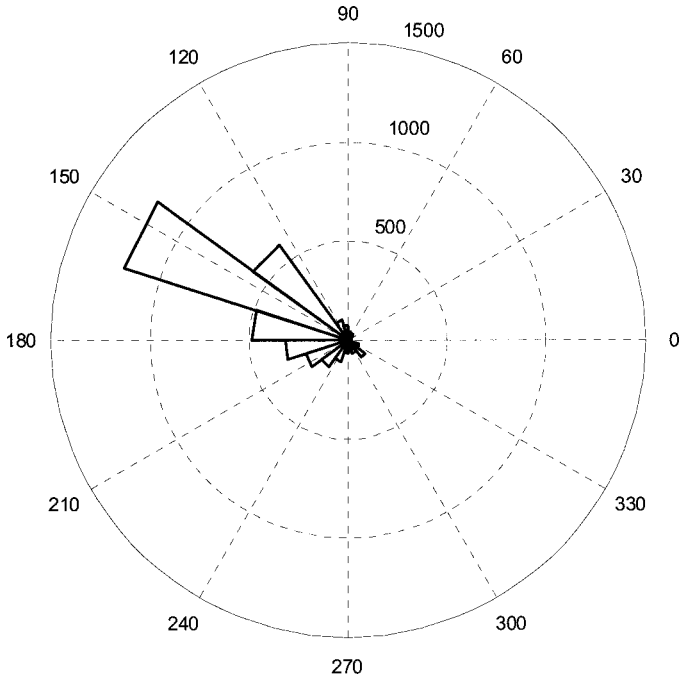

Fig. 2. The wind direction at Sedgwick Reserve between 10 February and 15 April 1997 through 2002 (in 1998, data are absent between 8 March and 20 April between 1100 and 1900 hours). The compass is divided into 12 intervals of 30° each. In each interval, the length of the wedge is proportional to the number of times the hourly mean wind direction came from that interval. Concentric circles indicate counts of 500, 1000, and 1500.

$\frac{1}{2}\pi$), a measure of anisotropy. The null hypothesis for this second test is that $r^{[h]}(\theta) = r^{[h]}(\text{isotropic}) = r^{[h]}(\theta \pm \frac{1}{2}\pi)$. In other words, we evaluate anisotropy as a deviation from isotropic pattern, whatever that might be. The test itself takes the form:

$$Z(\theta_{\max}) = \sqrt{\sum_{h=1}^{H} \frac{\left\{ r^{[h]}(\theta_{\max}) - r^{[h]}\left(\theta_{\max} \pm \frac{1}{2}\pi\right)\right\}^2}{\tilde{\sigma}^2_{\theta h}}}, \quad (5)$$

where $\tilde{\sigma}^2_{\theta h}$ is now the estimated variance of $r^{[h]}(\theta)$, under random permutation of the angular orientations of the paired genotypic observations in the $[h]$th distance class. Individual pairs are not permuted among intervals with this procedure, so isotropic ''structure'' is preserved. With random sampling alone, we should anticipate that there would always be some angle (θ), such that $r^{[h]}(\theta)$ would be maximized. We need to determine whether the observed pattern of anisotropy is more pronounced than a randomly generated pattern of anisotropy, i.e., to determine whether the ''directional signal is greater than the sampling noise.'' In addition to finding (and testing) the angle ($\theta_{\max}$) that optimized $Z(\theta_{\max})$, we have evaluated $Z(\theta_{\text{wind}})$ to determine whether prevailing wind direction accounts for any anisotropy encountered. If wind direction has an homogenizing effect on spatial structure, we should expect that $\theta_{\text{wind}} \sim \theta_{\max} \pm \frac{1}{2}\pi$.

RESULTS

Wind regime—During the flowering period, late afternoon wind speeds are typically 3.5–4.2 m/s, with maximum hourly averages of 7–9 m/s over the period of record (F. W. Davis, unpublished data). The wind rose for the hours 1100 to 1900 is comparable to that for the 24h period (F. W. Davis, unpublished data) and shows the strong directionality of winds from the west–northwest, i.e., from 292.5° (Fig. 2), which is true for most locations at low elevations in the Santa Ynez Valley (e.g., Ogden, 1975). Compared to the weather station, 900 m away and on flat terrain, wind speeds in the study area may be reduced slightly by the sheltering effect of local topography, but the direction should be much the same.

TABLE 1. Characteristics of the eight loci used in the *Q. lobata* population at Sedgwick Reserve. N_{all}, H_o, H_e, and F_{IS} are the number of observed alleles, the observed heterozygosity, the expected heterozygosity, and the fixation index for each locus, respectively. The *P* value is the probability that allelic frequencies departure from Hardy-Weinberg proportions. The mean is the average over the eight loci.

Locus	N_{all}	H_o	H_e	F_{IS}	*P*
MSQ4	21	0.86	0.87	0.01	0.60
QpZAG110	20	0.89	0.85	−0.05	0.63
Qm50	14	0.81	0.82	0.01	0.15
QpZAG 9	16	0.81	0.83	0.01	0.59
QpZAG 36	10	0.66	0.65	−0.01	0.15
QrZAG 20	9	0.62	0.59	−0.05	0.07
QpZAG 1/5	11	0.70	0.70	0.00	0.37
QrZAG 11	8	0.65	0.61	−0.06	0.27
Mean	13.6	0.75	0.74	−0.02	0.20

Genetic diversity within the Figueroa Creek population—The numbers of alleles ranged between 8 and 21 for the eight microsatellite loci we analyzed, and gene diversity (H_e) ranged between 0.64 for QrZAG11 and 0.87 for MSQ4 (Table 1). Outcross mating is essentially 100% for Valley oak (Sork et al., 2002b), but the majority of effective pollination would be localized (Sork et al., 2002a; Austerlitz et al., 2004), which could translate into small amounts of inbreeding due to mating between relatives growing in close proximity. We estimate the inbreeding coefficient to be slightly negative, averaged over loci ($F_{IS} = -0.02$; Table 1), however, indicating a small, but not significant, excess of heterozygotes. None of the single-locus exact tests for departures from Hardy-Weinberg proportions were significant (Table 1), nor was the overall test ($P = 0.20$), and single loci conformed reasonably well to Hardy-Weinberg proportions; there is no direct evidence for inbreeding in this population.

We did, however, detect significant departures from gametic equilibrium for 4 of 28 pairs of loci: QpZAG36–QpZAG1/5 ($P < 0.0001$), QpZAG110–QrZAG11 ($P < 0.01$), Qm50–QrZAG11 ($P < 0.05$), and QrZAG11–QrZAG20 ($P < 0.05$), though only the first survives Bonferroni adjustment for multiple tests. Studies in *Q. robur* (Barreneche et al., 1998) and *Castanea sativa*, another Fagaceous species (Barreneche et al., 2004), suggest that our microsatellite loci are unlinked. Nontrivial cross-locus disequilibria provide a longer-lasting signature of spatial subdivision within populations than do single-locus *F* coefficients (see Smouse et al., 1983; Epperson, 1995). Our methods for testing IBD and estimating σ assume independent loci, so we removed QrZAG11 and QpZAG1/5 for trial analyses, but the genetic signature for isolation by distance and multi-allelic dispersal estimates were not significantly affected (analyses not shown). On the premise that these loci are (probably) not physically linked and that the disequilibrium is probably due to the spatial pattern of IBD itself, we have chosen to retain all loci assayed.

Decrease of kinship coefficient with spatial distance—The average kinship coefficient decreased steadily with the natural logarithm of the distance separating individuals (Fig. 3). The

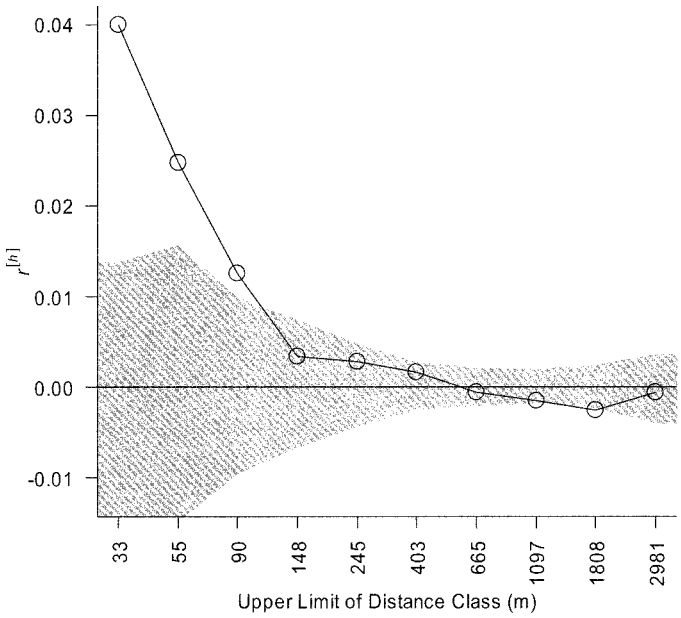

Fig. 3. Isotropic correlogram of relatedness among pairs of Valley oak (*Quercus lobata*) adults as a function of pairwise distance classes. $r^{[h]}$ is Nason's average kinship coefficient (Loiselle et al., 1995) over all pairs of individuals included in the spatial distance interval [*h*]. The upper limit of each interval [*h*] is given on the *x*-axis. The shaded areas indicate the 95% confidence band of the null hypothesis.

largest correlation occurred in the first distance class ($r^{[1]} = 0.042 \pm 0.016$), and $r^{[h]}$ became negative for the first time in the seventh distance class (i.e., for individuals separated by a distance ranging from 403 to 664 m) and remained negative in all the larger distance classes (Fig. 3). The first three *r* values (i.e., individuals separated by less than 90 m) were significantly more positive than expected in a random population ($P \leq 0.05$), in spite of the fact that larger confidence intervals were observed for the first three distance classes than for the others. The large confidence intervals were a predictable consequence of the fact that the numbers of pairs in these initial distance classes ($n_h = 108$–266) were smaller than those for the later distance classes ($n_h = 485$–5086). The multilocus correlogram (Fig. 3) shows strong divergence ($t = 5.8$; $P < 0.001$) from the null hypothesis of no autocorrelation.

Test of isolation by distance and gene flow estimates—When all pairs were used, the estimated regression slope was -0.0044 (± 0.0014), yielding $S_p = 0.0046$. The multilocus regression slope was significantly different from that obtained in a random population ($P < 0.001$) when all the pairs were considered. The estimates of S_p varied substantially across loci (Table 2), but the average regression slope translated into an estimate of $N_e = (4\pi D_e \sigma^2) = 215.9$ individuals. Setting $D_e = 0.000136$ individuals/m^2; (the census density of the sampling area), we obtained $\hat{\sigma} = 355$ m. The iterative procedure to estimate σ failed to converge when we set $D_e = 0.000136$ individuals/m^2, but when we used a value somewhat closer to the presumed historical reproductive density ($D_e = 0.0003$: F.W. Davis, unpublished data), the iterative procedure yielded an estimate of $\hat{\sigma} = 353$ m. Using only pairs included between 353 m and the maximum spatial distance (i.e., 2628 m), the regression slope was -0.0020 (± 0.0008) and was significantly different from that obtained in a random population ($P = 0.048$). The standard error of the slope yielded a 95% CI of $\hat{\sigma}$ that ranged between 263 and 853 m.

TABLE 2. Test of isolation by distance and estimates of gene dispersal in *Quercus lobata* using the multilocus procedure (all loci) and for each locus. The average kinship coefficient between individuals separated by the first distance class ($r^{[1]}$), the regression slope (b_k), the number of pairs (*N*) and the S_p statistic ($b_k/[F_1 - 1]$; see text for details) are given, considering all pairs. *P* is the type I error rate associated with the hypothesis of no isolation by distance (see Materials and Methods for details).

Locus	$r^{[1]}$	b_k	*N*	S_p	*P*
All loci	−0.042	−0.0044	18 145	0.0046	$<10^{-3}$
MSQ4	0.031	−0.0029	17 578	0.0030	0.045
QpZAG110	−0.04	−0.0029	18 145	0.0028	0.048
Qm50	0.068	−0.0056	15 753	0.0060	0.005
QpZAG9	0.035	−0.0038	17 766	0.0040	0.022
QpZAG36	−0.006	−0.0030	17 766	0.0030	0.110
QrZAG20	0.005	0.0000	18 145	0.0000	0.452
QpZAG1/5	0.120	−0.0137	18 145	0.0155	0.002
QrZAG11	0.068	−0.0028	18 145	0.0030	0.114

Directional autocorrelation—The correlograms along the wind azimuth ($\theta_{wind} = 292.5°/112.5°$) and across it ($\theta_{wind} \pm \frac{1}{2}\pi = 202.5°/22.5°$), are shown in Fig. 4a, where they are contrasted with the isotropic result and with the 95% confidence band for the isotropic reference case. Departure from the null hypothesis of isotropy [$r^{[h]}(\theta) = r^{[h]}(\text{isotropic}) = r^{[h]}(\theta \pm \frac{1}{2}\pi)$] is not significant for any one distance class, nor is the multiclass test criterion $Z(\theta_{wind}) = 4.57$, with $P \leq 0.53$. The angle of maximum anisotropy, as judged by the *Z* test, is actually ($\theta_{max} = 286°/106°$), running 6.5° "off the wind." The correlograms along the θ_{max} azimuth and across it ($\theta_{min} = 196°/16°$) are shown as Fig. 4b, again contrasted with the isotropic result and with the 95% isotropic confidence band. Clearly though, $Z(\theta_{max}) = 4.63$ ($P \leq 0.50$) is still not significant. No great meaning should be attached to the directional nuances of these results, since the cumulative evidence for anisotropy is itself subtle, but it is interesting to note that what little directional pattern there is lies roughly along the wind, rather than across it. The autocorrelogram itself decreases convincingly with distance ($P \leq 0.001$), but our analysis does not detect anisotropy. On balance, the isotropic treatment would seem to be an adequate description for these data.

DISCUSSION

Spatial genetic structure in Valley oak—The monotonic decline of the kinship coefficient with increasing spatial distance favors the hypothesis of historically restricted gene flow in Valley oak at the Figueroa Creek site. In particular, the high kinship coefficients for short distance classes (between 30 and 100 m; Fig. 3) are compatible with very restricted pollen and seed dispersal. Our results on pollination distance for two years (Sork et al., 2002a; Austerlitz et al., 2004) suggest that σ for pollination distance ranges between 50 and 88 m, substantially smaller than the historical estimate of ~350 m (for seed and pollen together).

Seed dispersal distance in *Q. lobata* is still not well known, but it is often assumed that seed movement is more restricted than pollen movement in oaks (Ducousso et al., 1993). What we do know is that acorns are removed by birds and rodents with different potential impact on dispersal distances. After

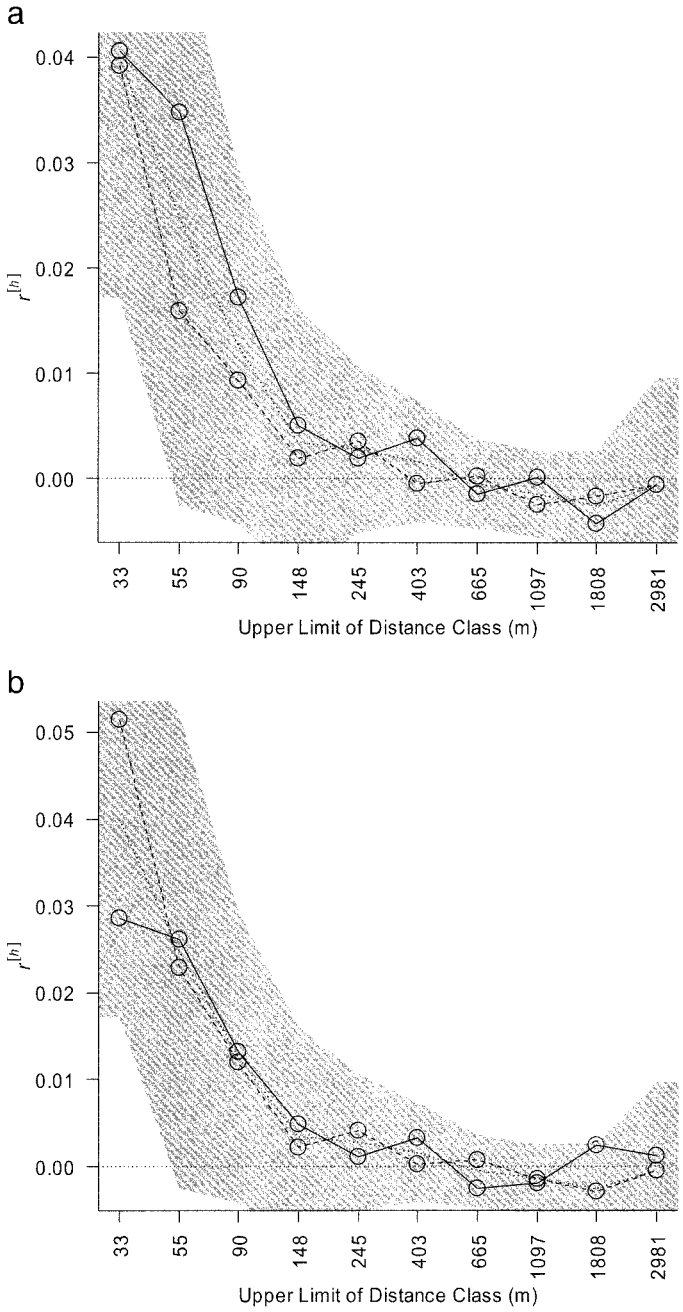

Fig. 4. Anisotropic correlogram of relatedness among pairs of Valley oak (*Quercus lobata*) adults, as a function of pairwise distance classes and the directional angle: (a) by distance, along the wind axis (θ_{wind} = 292.5° ↔ 112.5°, solid) and across the wind axis (θ = 202.5° ↔ 22.5°, dashed), compared with the isotropic (radially symmetric) correlogram (dotted); (b) by distance, along the angle of greatest anisotropy, as judged by the *Z* test (θ_{max} = 286° ↔ 106°, solid) and at right angles to the strongest axis (θ_{min} = 196° ↔ 16°, dashed), compared with the isotropic correlogram (dotted). $r^{[h]}$ is Nason's average kinship coefficient (Loiselle et al., 1995) over all the pairs of individuals included in the spatial distance interval [*h*]. The upper limit of each interval [*h*] is given on the *x*-axis. The shaded areas indicate the 95% confidence bands of the isotropic null hypothesis.

maturation, many acorns are removed from the canopy by acorn woodpeckers (*Melanerpes formicivorus*) and scrub jays (*Aphoelocoma coerulescens*) (Pavlik et al., 1991). Acorn woodpeckers can certainly fly for great distances (Koenig et al., 2000), but any dispersal they contribute is incidental loss en route to storing acorns in their granaries, located in their own territories (Pavlik et al., 1991). Acorns destined for the granary do not contribute to recruitment of Valley oak, and when they do, dispersal distances are not likely to be great (D. Grivet and V. Sork, unpublished data). Scrub jays, on the other hand, disperse acorns by planting them singly, and those that are not recovered may enter the population. Thus, scrub jays are capable of dispersing acorns, but their activities seem to be mostly local (V. Sork, personal observation) and little is known about frequency of long distance transport (Pavlik et al., 1991).

Remaining acorns fall to the ground, where active transport by small rodents, such as California ground squirrels (*Spermophilus beecheyi*) and deer mice (*Peromyscus maniculatus*), also comes into play. It is generally assumed that rodents are the principal dispersal agents but that seed dispersal is highly localized (Ducousso et al., 1993). When rodent-dispersed acorns become established seedlings, those individuals should create a pattern of local clustering of close relatives. Fine-scale genetic structure should be determined more by small-scale rodent-mediated seed dispersal than by occasional long-distance events, such as transport by jays. For this reason, Sork et al. (1993) ascribed the significant autocorrelation at short spatial scales in a United States Midwestern temperate oak species, *Quercus rubra*, to be the result of localized dispersal by rodents.

Our correlogram indicates low gene dispersal. It suggests that pollen and/or seed dispersal are restricted in *Q. lobata*, which is in agreement with our contemporary pollen estimate. Seed dispersal could contribute to produce this strong IBD pattern if jays and woodpeckers, although capable of long-distance dispersal, play a limited role on settlement of most seedlings. On the other hand, if most established seedlings are derived from rodent- or gravity-dispersed seed, we would expect clusters of relatives and a resulting pattern of IBD that is consistent with the autocorrelated spatial structure we observe.

The decay of kinship with increasing log (distance) was nonlinear, with the curve becoming less steep beyond 100 m (Fig. 3). Values of kinship in the shortest spatial intervals are sensitive to the precise parametric form of the dispersal function, which can explain the nonlinearity of the regression over the entire range of distances (Rousset, 1997; Hardy and Vekemans, 1999). Strong kurtosis of the dispersal function, unequal dispersal distributions for seed and pollen, small values of ($D_e\sigma^2$), and/or low migration rates among populations all produce a high kinship coefficient between proximal pairs of individuals, followed by a rapid decrease in kinship for more distant individuals (Hardy and Vekemans, 1999; Heuertz et al., 2003; Vekemans and Hardy, 2004).

In this oak savanna setting, densities of less than 3 individuals/ha since the 19th century could have promoted small values of $D_e\sigma^2$, if gene flow was spatially restricted. If seed dispersal is substantially more limited than wind-mediated pollen dispersal, then the difference should also produce a highly nonlinear kinship correlogram (Heuertz et al., 2003). Furthermore, contemporary pollen-dispersal curves were estimated leptokurtic in *Q. lobata* (Austerlitz et al., 2004), which should

reinforce this shape of the correlogram if historical dispersal has not been strongly modified by demographic change.

Spatial genetic structure has been reported in other oak species from North America (*Quercus rubra*, Sork et al., 1993; *Q. laevis*, Berg and Hamrick, 1995), Europe (*Q. petrea* and *Q. robur*, Streiff et al., 1998), and Asia (*Q. acutissima*, Chung et al., 2002). For these species, however, significant genetic structures were observed over shorter distances (<30 m), and kinship coefficients were either nonsignificant or smaller than we see here for *Q. lobata*. Direct comparisons of relationship coefficients across studies should be made with some caution, of course, because they are sensitive to the spatial scales investigated (Dutech et al., 2002; Fenster et al., 2003), to the methods used (Smouse and Peakall, 1999), and to the genetic markers analyzed (Streiff et al., 1998). That is why we have used the S_p statistic of Vekemans and Hardy (2004), which is equivalent to $1/4\pi D_e\sigma^2$, as a convenient parametric representation for comparison of spatial genetic structure among species.

The S_p value we found for *Q. lobata* ($S_p = 0.0046$) is intermediate between those found for *Q. robur* ($S_p = 0.003$) and *Q. petraea* ($S_p = 0.008$) by Vekemans and Hardy (2004), who also indicate a negative correlation between S_p and the effective population density. Valley oak, with an adult density of 1–3 individuals/ha, should exhibit a stronger genetic structure than other European and North American oaks, for which adult densities are generally greater than 50 adults/ha. As pointed out by Vekemans and Hardy (2004), however, low-density species may exhibit increased distances of gene movement, due to the greater pollination distances between reproductive individuals. For example, our savanna population of Valley oak yields an estimate of $\hat{\sigma} = 50$ m (Sork et al., 2002a), greater than that observed for a high-density forest population of *Q. alba* ($\hat{\sigma} = 9$ m; Smouse et al., 2001). This inter-tree distance effect and the openness of canopy in the savanna could explain why Valley oak, in spite of its lower adult density, has less spatial genetic structure than *Q. petraea*.

Gene flow estimates—We can assess the hypothesis of low gene flow with an estimate of neighborhood size ($4\pi D\sigma^2$) from the regression slope. If we consider the census density of 3 individuals/ha (the historical tree density at the approximate time that this cohort was established), σ can be estimated as 353 m, using the iterative procedure of Fenster et al. (2003). This estimate, which combines pollen and seed-mediated gene flow, was definitely larger than the indirect σ estimate of contemporary pollen dispersal provided by TWOGENER analysis (i.e., between 50 m and 90 m: Sork et al., 2002a; Austerlitz et al., 2004).

It is difficult to be certain whether the discrepancy is due to the assumptions and statistical nuances of the two approaches or whether the scale of gene flow has actually changed. Our contemporary and historical estimates should be taken with caution because they both have large variances and assumptions that affect the estimates. On one hand, the contemporary estimate assumes a specific dispersal curve (see Austerlitz et al., 2004) and an estimate of current adult density that may be higher than the effective reproductive adult density. Either or both of these assumptions could lead to an underestimate of neighborhood area (Austerlitz et al., 2004). On the other hand, the estimate of historical gene flow assumes migration/genetic drift equilibrium (e.g., Hardy and Vekemans, 1999) but climatic change in California during the last few centuries may have created demographic disequilibrium. Thus, historical gene flow could be overestimated if demographic disturbances have eroded spatial genetic structure (see for example Knowles et al., 1992).

To the extent that the perceived difference is real, two nonexclusive hypotheses can be invoked to explain the difference: (1) Seed flow is much less spatially restricted then previously assumed, and if contemporary estimates of seed-mediated σ were included in an overall σ, the difference in the two estimates would disappear or be reduced. While our current observations on acorn movements by rodents, acorn woodpeckers, and jays are still limited (D. Grivet and V. L. Sork, unpublished data), it seems unlikely that seed dispersal is more than twice as extensive as pollen dispersal. (2) Contemporary pollen flow has been reduced by the decrease in reproductive density in *Q. lobata* in post-colonial times, due to continuous demographic attrition. Although decreasing density can promote pollen dispersal (see INTRODUCTION), demographic attrition should also promote a proportionately greater degree of mating among proximal individuals, reducing the value of σ for pollen dispersion as suggested for *Q. lobata* (Sork et al., 2002a). We have studies of both seed and pollen dispersal, currently in progress at Sedgwick Reserve, that should shed some additional light on these issues.

Impact of wind direction on genetic structure and dispersal estimates—For this study site (and the region in general), the predominant wind direction is from the west–northwest during the pollination period of Valley oak. Our analysis of anisotropy yields a maximum *Z* value along the 286°/106° azimuth, close to the predominant wind direction of 295.5°/112.5°. Even our best anisotropic model was far from significant, however, and we expect the correlogram to be steeper across the wind axis than along it, the reverse of what pattern we do see. Perhaps it is not surprising that we do not see the signature of the wind in our adult spatial genetic structure. First, seed dispersal, which probably has no wind component, could dilute any such effect. Moreover, by the time the established individuals were assayed as adults, 100–300 years after germination, micro-local selection pressures and random demographic losses could have overwhelmed any initial wind signature. Studies of the pattern of wind-mediated pollen movement are still under way, but it will be interesting to see whether contemporary pollen movement itself is detectably anistotropic.

In summary, we show significant autocorrelation in the Valley oak population at Sedgwick Reserve, with a strong signal of shared genetic affinity, particularly for pairs of individuals separated by short distances (less than 100 m). Using regression methods, we estimate that the historical standard deviation of the propagule dispersal distribution is on the order of 350 m (for pollen and seed combined). Contrary to expectation, however, the Sedgwick Reserve population of Valley oak yields no more than a hint of historically anisotropic gene flow, in spite of strong prevailing winds from the west–northwest during the pollination period. This latter finding indicates either that the wind has had limited effect on pollen flow or that seed flow and subsequent demographic factors, playing out over several decades, have overwhelmed any initial ''wind-signature.''

This study is unique in its comparison of historical and contemporary gene flow for the same population. The spatial signature of past gene flow provides a useful reference against

which to gauge the future consequences of contemporary processes. Additional studies of contemporary pollen and seed flow that will shed light on these issues are currently in process, but the results reported here suggest that contemporary gene flow could be more restricted than has been true in the past and that further demographic attrition and fragmentation of the extant Valley oak population, a probable consequence of ongoing anthropogenic disturbance, can further decrease the level and extent of gene flow across California's savanna oak landscape.

LITERATURE CITED

AUSTERLITZ, F., C. DICK, C. DUTECH, E. K. KLEIN, S. ODDOU-MURATORIO, P. E. SMOUSE, AND V. L. SORK. 2004. Using genetic markers to estimate the pollen dispersal curve. *Molecular Ecology* 13: 937–954.

BARRENECHE, T., C. BODENES, C. LEXER, J. F. TRONTIN, S. FLUCH, R. STREIFF, C. PLOMION, G. ROUSSEL, H. STEINKELLNER, K. BURG, J. M. FAVRE, J. GLÖSSL, AND A. KREMER. 1998. A genetic linkage map of *Quercus robur* L. (pedunculate oak) based on RAPD, SCAR, microsatellite, minisatellite, isozyme and 5S rDNA markers. *Theoretical and Applied Genetics* 97: 1090–1103.

BARRENECHE, T., M. CASASOLI, K. RUSSELL, A. AKKAK, H. MEDDOUR, C. PLOMION, F. VILLANI, AND A. KREMER. 2004. Comparative mapping between *Quercus* and *Castanea* using simple-sequence repeats (SSRs). *Theoretical and Applied Genetics* 108: 558–566.

BERG, E. E., AND J. L. HAMRICK. 1995. Fine-scale genetic structure of a turkey oak forest. *Evolution* 49: 110–120.

BROWN, R. W., AND F. W. DAVIS. 1991. Historic mortality of valley oak in the Santa Ynez Valley, Santa Barbara County, CA. *In* R. Standiford [ed.], Proceedings of the Symposium on Oak Woodlands and Hardwood Rangeland Management, 31 October–2 November 1990, USDA Forest Service General Technical Report PSW-126, 202–207. Albany, California, USA.

CHUNG, M. Y., J. NASON, M. G. CHUNG, K.-J. KIM, C.-W. PARK, B.-Y. SUN, AND J.-H. PAK. 2002. Landscape-level spatial genetic structure in *Quercus acutissima* (Fagaceae). *American Journal of Botany* 89: 1229–1236.

DICK, C. W., G. ETCHELECU, AND F. AUSTERLITZ. 2003. Pollen dispersal of tropical trees (*Dinizia excelsa*: Fabaceae) by native insects and African honeybees in pristine and fragmented Amazonian rainforest. *Molecular Ecology* 12: 753–764.

DORMAN, C. E., AND C. D. WINANT. 2000. The structure and variability of the marine atmosphere around the Santa Barbara Channel. *Monthly Weather Review* 128: 261–282.

DOW, B. D., M. V. ASHLEY, AND H. F. HOWE. 1995. Characterization of highly variable (GA/CT)n microsatellites in the bur oak, *Quercus macrocarpa*. *Theoretical and Applied Genetics* 91: 137–141.

DUCOUSSO, A., H. MICHAUD, AND R. LUMARET. 1993. Reproduction and gene flow in the genus *Quercus* L. *Annales des Sciences Forestières* 50 (Suppl.): 91s–106s.

DUTECH, C., J. SEITER, P. PETRONELLI, H. I. JOLY, AND P. JARNE. 2002. Evidence of low gene flow in a neotropical tree species in two forest stands of French Guiana. *Molecular Ecology* 11: 725–738.

ELLSTRAND, N. C., AND D. R. ELAM. 1993. Population genetic consequences of small population size: implications for plant conservation. *Annual Review of Ecology and Systematics* 24: 217–242.

ENNOS, R. A. 1994. Estimating the relatives rates of pollen and seed migration among plant populations. *Heredity* 72: 250–259.

EPPERSON, B. K. 1995. Fine-scale spatial structure: correlations for individual genotypes differ from those for local gene frequencies. *Evolution* 49: 1022–1026.

FAIRLEY, D., AND G. L. BATCHELDER. 1986. A study of oak-pollen production and phenology in northern California: prediction of annual variation in pollen counts based on geographic and meterologic factors. *Journal of Allergy and Clinical Immunology* 78: 300–307.

FENSTER, C. B., X. VEKEMANS, AND O. J. HARDY. 2003. Quantifying gene flow from spatial genetic structure data in a metapopulation of *Chamaecrista fasciculata* (Leguminosae). *Evolution* 57: 995–1007.

GRIFFIN, J. R. 1971. Oak regeneration in the upper Carmel Valley, California. *Ecology* 52: 862–868.

HARDY, O. J. 2003. Estimation of pairwise relatedness between individuals and characterization of isolation-by-distance processes using dominant genetic markers. *Molecular Ecology* 12: 1577–1588.

HARDY, O. J., AND X. VEKEMANS. 1999. Isolation by distance in a continuous population: reconciliation between spatial autocorrelation analysis and population genetics models. *Heredity* 83: 145–154.

HARDY, O. J., AND X. VEKEMANS. 2002. SPAGeDi: a versatile computer program to analyse spatial genetic structure at the individual or population levels. *Molecular Ecology Notes* 2: 618–620.

HEUERTZ, M., X. VEKEMANS, J. F. HAUSMAN, M. PALADA, AND O. J. HARDY. 2003. Estimating seed vs. pollen dispersal from spatial genetic structure in the common ash. *Molecular Ecology* 12: 2483–2495.

HEYWOOD, J. S. 1991. Spatial analysis of genetic variation in plant populations. *Annual Review of Ecology and Systematics* 22: 335–355.

ISAGI, Y., AND S. SUHANDONO. 1997. PCR primers amplifying microsatellite loci of *Quercus myrsinifolia* Blume and their conservation between oak species. *Molecular Ecology* 6: 897–899.

KNOWLES, P., D. PERRY, AND H. A. FOSTER. 1992. Spatial genetic structure in two tamarack (*Larix laricinia* (du roi) K. Koch) populations with differing establishment histories. *Evolution* 46: 572–576.

KOENIG, W. D., P. N. HOOGE, M. T. STANBACK, AND J. HAYDOCK. 2000. Natal dispersal in the cooperatively breeding Acorn Woodpecker. *Condor* 102: 492–502.

LEDIG, F. T. 1988. The conservation of diversity in forest trees. *BioScience* 38: 471–479.

LEDIG, F. T. 1992. Human impacts on genetic diversity in forest ecosystems. *Oikos* 63: 87–108.

LOISELLE, B. A., V. L. SORK, J. NASON, AND C. GRAHAM. 1995. Spatial genetic structure of tropical understory shrub, *Psychotria officinalis* (Rubiaceae). *American Journal of Botany* 82: 1420–1425.

MALÉCOT, G. 1950. Quelques schémas probabilistes sur la variabilité des populations naturelles. *Annales de l'Université de Lyon A* 13: 37–60.

NASON, J. D., AND J. L. HAMRICK. 1997. Reproductive and genetic consequences of forest fragmentation: two case studies of Neotropical canopy trees. *Journal of Heredity* 88: 264–276.

NEI, M. 1987. Molecular evolutionary genetics. Columbia University Press, New York, New York, USA.

ODEN, N. L., AND R. R. SOKAL. 1986. Directional autocorrelation: an extension of spatial correlograms to two dimensions. *Systematic Zoology* 35: 608–617.

OGDEN, G. L. 1975. Differential response of two oak species to far inland advection of sea-salt spray aerosol. Ph.D. dissertation, University of California, Santa Barbara, California, USA.

PAVLIK, B. M., P. C. MUICK, S. G. JOHNSON, AND M. POPPER. 1991. Oaks of California. Cashuma Press and The California Oak Foundation, Los Olivos, California, USA.

RAYMOND, M., AND F. ROUSSET. 1995. GENEPOP (version 1.2): population genetics software for exact tests and ecumenicism. *Journal of Heredity* 86: 248–249.

ROCHA, O. J., AND G. AGUILAR. 2001. Reproductive biology of the dry forest tree *Enterolobium cyclocarpum* (Guanacaste) in Costa Rica: a comparison between trees left in pastures and trees in continuous forest. *American Journal of Botany* 88: 1607–1614.

ROSENBERG, M. 2000. The bearing correlogram: a new method of analyzing directional spatial autocorrelation. *Geographical Analysis* 32: 267–278.

ROUSSET, F. 1996. Equilibrium values of measures of population subdivision for stepwise mutation processes. *Genetics* 142: 1357–1362.

ROUSSET, F. 1997. Genetic differentiation and estimation of gene flow from F-statistics under isolation by distance. *Genetics* 145: 1219–1228.

ROUSSET, F. 2000. Genetic differentiation between individuals. *Journal of Evolutionary Biology* 13: 58–62.

SLATKIN, M. 1987. Gene flow and the geographic structure of natural populations. *Science* 236: 787–792.

SMOUSE, P. E., R. J. DYER, R. D. WESTFALL, AND V. L. SORK. 2001. Two-generation analysis of pollen flow across a landscape. I. Male gamete heterogeneity among females. *Evolution* 55: 260–271.

SMOUSE, P. E., J. V. NEEL, AND W. LIU. 1983. Multiple-locus departures from panmictic equilibrium within and between village gene pools of Amerindian tribes at different stages of agglomeration. *Genetics* 104: 133–153.

SMOUSE, P. E., AND R. PEAKALL. 1999. Spatial autocorrelation analysis of individual multiallele and multilocus genetic structure. *Heredity* 82: 561–573.

SMOUSE, P. E., AND V. L. SORK. 2004. Measuring pollen flow in forest trees:

an exposition of alternative approaches. *Forest Ecology and Management* 197: 21–38.

SORK, V. L., F. W. DAVIS, P. E. SMOUSE, V. J. APSIT, R. J. DYER, J. F. FERNANDEZ, AND B. KUHN. 2002a. Pollen movement in declining populations of California Valley oak, *Quercus lobata*: where have all the fathers gone? *Molecular Ecology* 11: 1657–1668.

SORK, V. L., R. J. DYER, F. W. DAVIS, AND P. E. SMOUSE. 2002b. Mating patterns in a savanna population of valley oak (*Quercus lobata* Neé). *In* R. Standiford, D. McCreary, and K. L. Purcell [eds.], Fifth Symposium on Oak Woodlands: Oaks in California's Changing Landscape, 22–25 October 2001, USDA Forest Service General Technical Report, PSW-GTR-184, 427–439. San Diego, California, USA.

SORK, V. L., S. HUANG, AND E. WIENER. 1993. Macrogeographic and fine-scale genetic structure in a North American oak species, *Quercus rubra* L. *Annales des Sciences Forestières* 50 (Suppl.): s261–s270.

SORK, V. L., J. NASON, D. R. CAMPBELL, AND J. F. FERNANDEZ. 1999. Landscape appoaches to historical and contemporary gene flow in plants. *Trends in Evolution and Ecology* 14: 219–224.

STEINKELLNER, H., S. FLUSH, E. TURETSHEK, C. LEXER, R. STREIFF, A. KREMER, K. BURG, AND J. GLÖSSL. 1997. Identification and characterization of $(GA/TC)_n$- microsatellite loci from *Quercus petraea*. *Plant Molecular Biology* 33: 1093–1096.

STREIFF, R., T. LABBÉ, R. BACILIERI, H. STEINKELLNER, J. GLÖSSL, AND A. KREMER. 1998. Within-population genetic structure in *Quercus robur* L. and *Quercus petraea* (Matt.) Liebl. assessed with isozymes and microsatellites. *Molecular Ecology* 7: 317–328.

TUFTO, J., S. ENGEN, AND K. HINDAR. 1997. Stochastic dispersal processes in plant populations. *Theoretical Population Biology* 52: 16–26.

VEKEMANS, X., AND O. J. HARDY. 2004. New insights from fine-scale spatial genetic structure analyses in plant populations. *Molecular Ecology* 13: 931–935.

WEIR, B. S., AND C. C. COCKERHAM. 1984. Estimating F-statistics for the analysis of population structure. *Evolution* 8: 1358–1370.

WRIGHT, S. 1943. Isolation by distance. *Genetics* 28: 114–138.

WRIGHT, S. 1951. The genetical structure of populations. *Annals of Eugenics* 15: 323–354.